

SIMULATION AND MEASUREMENT OF BEAM LOADING EFFECTS IN MAGNETIC ALLOY RF CAVITY OF CSNS RCS

Hanyang Liu, Liangsheng Huang, Yang Liu, Shouyan Xu, Sheng Wang*

Institute of High Energy Physics, Beijing, China

Spallation Neutron Source Science Center, Dongguan, Guangdong, China

Abstract

Different from the ferrite cavity, the Q value of magnetic alloy cavity in CSNS RCS is only about 1.25, the frequency band of impedance is wide, and the beam loading effects is strong. Based on the impedance measurement results, the influence of the beam load effects on the longitudinal distribution of the magnetic alloy cavity in CSNS RCS is studied by simulation, and the induced voltage measured on the machine is consistent with it.

INTRODUCTION

The average beam power of 125 kW has been achieved in February 2022, 25% more than the designed power. In order to further improve the beam power, a magnetic alloy (MA) material rf cavity [1] was added to the rapid cycling synchrotron (RCS) during the summer maintenance in 2022 to form a double harmonic system with the ferrite cavity, so as to improve the longitudinal beam distribution, increase the bunching factor and mitigate the space charge effects in the first few milliseconds. Compared to the ferrite cavity, MA cavity has a higher accelerating voltage gradient and the lower Q value gives it a wider bandwidth, eliminating the need for an additional tuning system. However, the beam loading effect of MA cavities is very serious, which should be considered carefully in high-intensity proton synchrotrons [2, 3]. In order to reduce the beam loading effects, a feedback system is used in the MA cavity to compensate for the induced voltage. In this paper, the measured impedance is used to simulate the beam loading effects using PyORBIT [4], and some customized functions have been added to meet the requirements of the simulation [5]. The induced voltage in MA cavity has been also measured.

MEASUREMENT AND SIMULATION

The wake voltage due to the beam loading effects is expressed as

$$V_{cavity}(\omega) = Z_{cavity}(\omega) \cdot I_{beam}(\omega)$$

where V_{cavity} and I_{beam} are the wake voltage and beam current at the frequency ω . The impedance Z_{cavity} of MA cavity per half gap is given in Fig. 1, which is measured by the coaxial-wire method [6, 7]. The impedance Z_{cavity} can be represented in the LRC model, which is

$$Z_{cavity}(\omega) = \frac{R_L}{1 - iQ_L(\frac{\omega_r}{\omega} - \frac{\omega}{\omega_r})}$$

* wangsh@ihep.ac.cn

where the shunt resistance R_L is 196.7 Ω , the resonate frequency ω_r is 2.06 MHz, the quality factor Q_L is about 1.25. The main RCS parameters are shown in the Table. 1

Table 1: RCS Main Parameter

Parameter	Value
Circumference	227.92 m
Harmonic number	2 / 4
Accelerating frequency	1.022- 2.444 MHz
Repetition	25 Hz
Maximum RF voltage	180 / 50 kV
Energy	0.08 – 1.6 GeV
Gap number of cavity	3
Particle number per bunch	1.092×10^{13} ppp

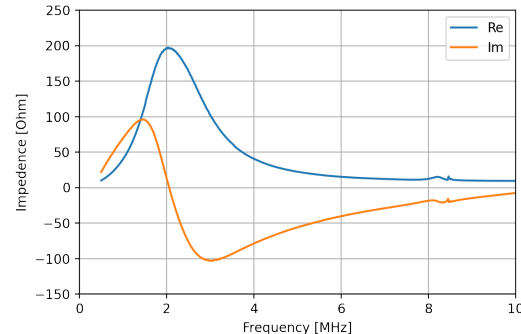


Figure 1: The real (blue) and imaginary (yellow) part of the measured impedance corresponding to the half gap of MA cavity.

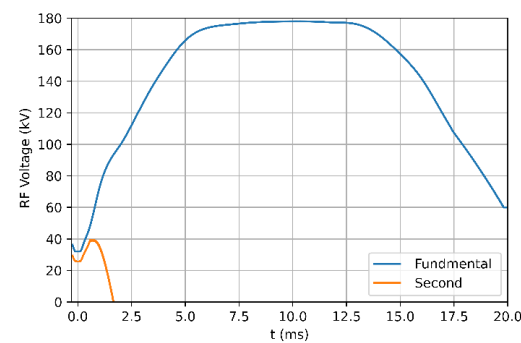


Figure 2: Fundamental harmonic(blue) and second harmonic(orange) voltage curve in 20 ms.

To evaluate the importance of beam loading compensation, the simulation has been taken with and without beam loading effects, and the rf curve is shown as Fig. 2. The longitudinal phase space at 20 ms with the beam loading effect is shown as the upper one of Fig. 3, which can be seen that the length of the beam increases slightly and its energy has a significant shift compare to the one without considering beam loading effect. Both the longitudinal phase spaces with and without the beam loading effect are matched to the bucket after the injection.

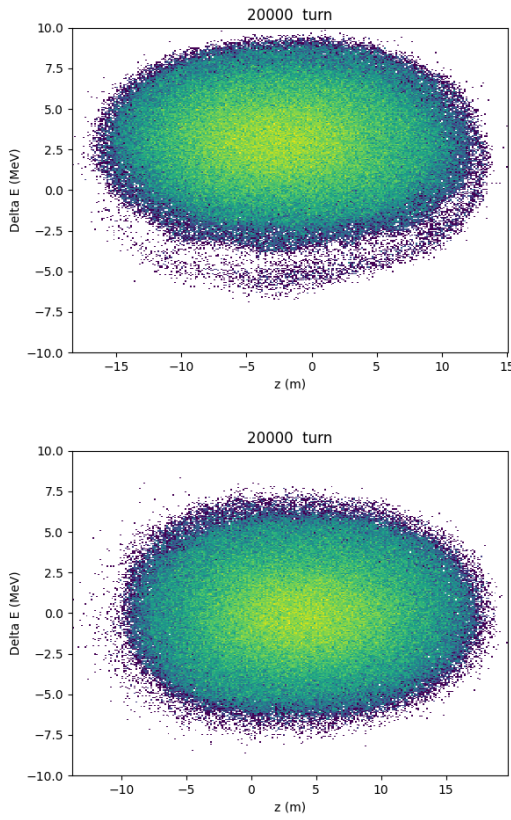


Figure 3: Comparison of the longitudinal phase space at extraction stage with (top) and without (bottom) beam loading effects in the simulation.

In order to verify the accuracy of the calculation, the original signal of the gap voltage has been measured as shown in Fig. 4. Since the cavity was not driven, the gap voltage consists of only the wake voltage. The four-transistor amplifier of MA cavity works on the push-pull mode, and the conversion formular of the gap voltage is

$$(gap\ voltage[V]) = \frac{([V_a\ [V]] + [V_b\ [V]])}{(1.8 \times 10^3)}$$

in which V_a and V_b is the amplitude of tank A and tank B, and the constant 1.8×10^3 is the conversion coefficient. The magnitude of the RF voltage displayed in the Fig. 4 is the value processed by the algorithm of the low-level rf (LLRF) control system. The maximum harmonic wake voltage values of the $h=2$ to $h=8$ excited are about 10 kV, 3 kV, 1 kV

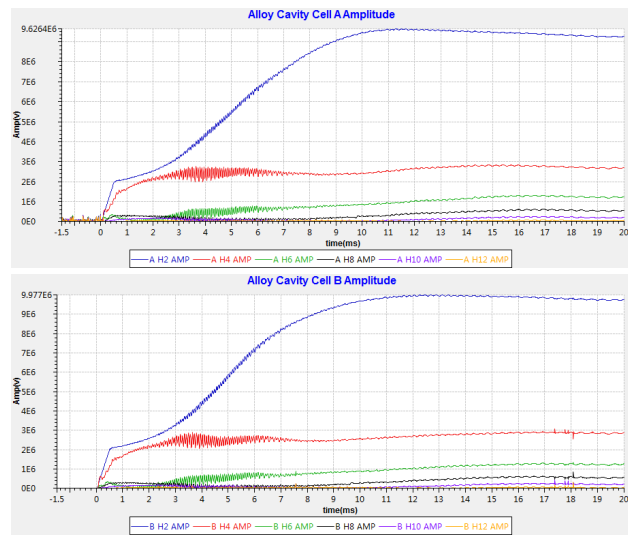


Figure 4: The harmonic components of wake voltage in MA cavity. Only the fundamental cavity voltage is used during the measurement.

and 0.5 kV, which is consistent with the simulation results as shown in Fig. 5. After using multiharmonic compensation through the feedback system of LLRF, all the components can be less than 0.5 kV.

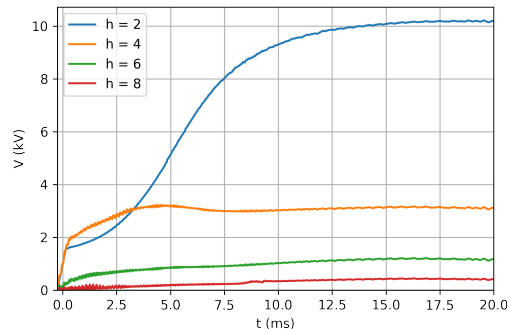


Figure 5: The wake voltage at different harmonic components. Only the fundamental cavity voltage is used in the simulation.

The parasitic impedance at 21.6 MHz has also been found from measurement, as shown in Fig. 6. Although the impedance value is large, its frequency is far from the fundamental frequency and the harmonic components of beam current are weak. The simulation result as Fig. 7 shows that all the components of the wake voltage are less than 0.8 kV in 20 ms, which have negligible influence on the beam current at this stage.

Considering the CSNS-II [5], more than 5 times the beam intensity of CSNS and two more MA cavities installed, the effects can be more serious. And the range of accelerating frequency in CSNS-II, which is from 1.717 to 2.444 MHz, is narrower than the one in CSNS. This makes the beam keep some higher harmonic components for a longer period of

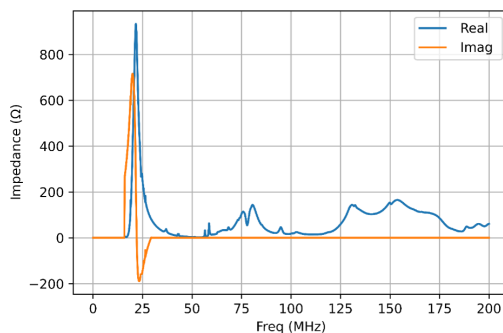


Figure 6: Parasitic impedance at 21.6 MHz

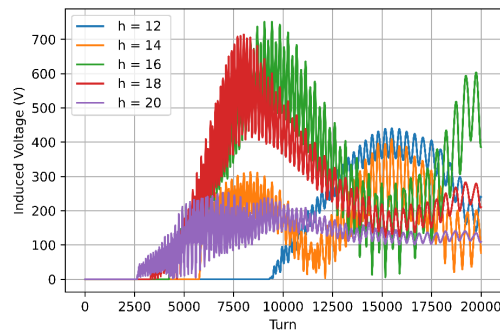


Figure 7: The wake voltage of parasitic impedance in CSNS.

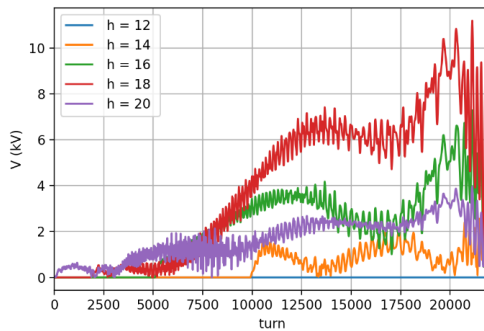


Figure 8: The wake voltage of parasitic impedance in CSNS-II.

time during the accelerating, which can also exacerbate the effects of parasitic impedance. The wake voltage in CSNS-II is shown as Fig. 8, in which the injection energy is 300 MeV and the particle number is 7.8×10^{13} ppp for a single bunch. It can be seen that the wake voltage increases significantly and that $h=14, 16, 18, 20$ all reach the kV magnitude at the extraction stage. Fig. 9 shows that the wake voltage will distort the phase space distribution, however the maximum bunch length doesn't increase compared to the one without this impedance. The effects in higher beam power are further being studied.

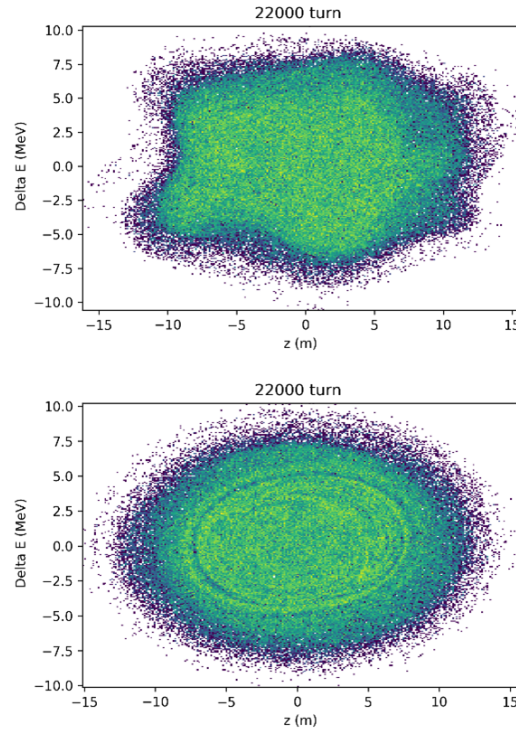


Figure 9: Comparison of the longitudinal phase space at extraction stage with (up) and without (down) beam loading effects in CSNS-II.

SUMMARY

We measure the impedance of the MA cavity by the coaxial-wire method and simulate its beam loading effects with PyORBIT. The shunt resistance R_L is 196.7 Ω, the resonant frequency ω_r is 2.06 MHz, the quality factor Q_L is about 1.25 and the maximum harmonic wake voltage values of the $h=2$ to $h=8$ excited are about 10 kV, 3 kV, 1 kV and 0.5 kV, which is consistent with the simulation results. A parasitic impedance of 21.6 MHz was also found from measurement, which has negligible influence on the beam current at this stage. However, with the increase of beam power, the influence of parasitic impedance will be amplified and may become one of the sources of instability.

ACKNOWLEDGEMENTS

We would like to thank all the CSNS ring rf group members for the helpful discussions and comments. This work is jointly supported by the National Natural Science Foundation of China (Project No. 12075134) and the Guangdong Basic and Applied Basic Research Foundation (Project No. 2021B1515120021).

REFERENCES

[1] B. Wu, H. Sun, X. Li, C. L. Zhang, and J. Y. Zhu, "Higher harmonic voltage analysis of magnetic-alloy cavity for CSNS/RCS upgrade project". *Radiat. Detect. Technol. Methods*, vol. 4, pp. 293–302, Sep. 2020. doi:10.1007/s41605-020-00183-z

[2] F. Tamura *et al.*, “Multiharmonic vector rf voltage control for wideband cavities driven by vacuum tube amplifiers in a rapid cycling synchrotron”, *Phys. Rev. Accel. Beams*, vol. 22, Sep. 2019. doi:10.1103/PhysRevAccelBeams.22.092001

[3] F. Pedersen, “Beam Loading Effects in the CERN PS Booster”, *IEEE Trans. Nucl. Sci.*, vol. 22, pp. 1906-1909, 1975. doi:10.1109/TNS.1975.4328024

[4] A. Shishlo, S. Cousineau, J. Holmes, and T. Gorlov, “The Particle Accelerator Simulation Code PyORBIT”, *Procedia Comput. Sci.*, vol. 51, pp. 1272-1281. 2015. doi:10.1016/j.procs.2015.05.312

[5] H. Liu and S. Wang, “Longitudinal beam dynamic design of 500 kW beam power upgrade for CSNS-II RCS”, *Radiat. Detect. Technol. Methods*, vol. 6, pp. 339-348. 2022. doi:10.1007/s41605-022-00325-5

[6] F. Caspers, “Bench methods for beam-coupling impedance measurement”, *Frontiers of Particle Beams: Intensity Limitations*, Berlin, Germany, 1992. doi:10.1007/3-540-55250-2_27

[7] L.-S. Huang *et al.* “Impedance measurements of the extraction kicker system for the rapid cycling synchrotron of China Spallation Neutron Source”, Supported by National Natural Science Foundation of China (11175193, 11275221). *Chinese Physics C*, 40(4). doi:10.48550/arXiv.1504.01500